Testing a new channel routing component in JGrass-NewAge model

Giuseppe Formetta
University of Trento, 77 Mesiano St., Trento, 38123

Olaf David
Dep. of Civil and Environmental Engineering, CSU, Fort Collins

Riccardo Rigon
University of Trento, 77 Mesiano St., Trento, 38123

Abstract. The paper presents two applications of the JGrass-NewAge model in order to investigate the influence of an explicit channel routing model on the discharge simulation. The semi-distributed, component based hydrological model JGrass-NewAge is based on the Object Modeling System version 3.0 (OMS3). OMS3, which facilitates exchange of model components, was used to set up two different model configurations named Hymod and RHymod, respectively. The two models differ only by the new channel routing component. Different basin delineations (one, three and twenty Hydrological Response Units (HRU)) are analyzed for both the model configurations. Simulated discharges in all the cases are compared with measurements from a quantitative point of view by using classical indices of goodness of fit such as index of agreement, percentage bias and Kling-Gupta efficiency.

1. NewAge-JGrass model

The model used in the applications presented in this paper is the NewAge-JGrass system (Formetta et al. (2011)): a system for hydrological cycle simulation at the basin scale. It includes different components dealing with estimation of different hydrological processes such as the space-time structure of precipitation, evapotranspiration, runoff production, aggregation and propagation of flows in channel, and automatic calibration of each model with different methods. The system is based on a hillslope-link geometrical partition of the landscape, so the basic unit for the water budget evaluation is the hillslope. Each hillslope drains into a single associated link rather than cells or pixels. This conceptual partition is developed using informatics with vector features for channels and raster data for hillslopes. Each model is a component, according to the definitions of the OMS3 (http://javaforge.com/wiki/57375; David et al. (2010) and can be substituted easily by others at run time without rewriting the whole code.

The model requires interpolation of meteorological variables (air temperature, precipitation, relative humidity) as input data for each hillslope. It can be handled by a deterministic (Inverse distance weighted (Cressie (1992), Goovaerts (1997), Lloyd (2005))), geostatistic (Goovaerts (1997)) or detrended Kriging (Garen et al. (1994) and Garen and Marks (2005)) approach. As a result, time series for required meteorological variables are generated for each hillslope.

The energy model, Formetta and Rigon (2011), includes both shortwave and longwave radiation components calculations for each hillslope. The shortwave radiation balance (beam and diffuse components) is described in Iqbal (1983), Bird and Hulstrom (1981) and Corripio (2002). The latter implements algorithms that take into account shade and complex topography. Shortwave radiation under generic sky conditions (all-sky) is computed according to Helbig et al. (2010) and using different parameterizations choices such as Erbs et al. (1982), Reindl et al. (1990) and Orgill and Hollands (1977). The longwave radiation budget is based on Brutsaert (1982) and Brutsaert (2005). After computing the net radiation for each hillslope, evapotraspiration can be modelled using three different solutions: the Fao-Evapotraspiration model (Allen et al. (1998)), the Penman-Monteith model (Penman (1948); Monteith et al. (1965)) the Priestley-Taylor model (Priestley (1959), Slatyer and McIlroy (1961), Priestley and Taylor (1972))).

The user can choose between two different runoff generation models: Duffy's model (Duffy (1996)) and Hymod model (Moore (1985); Boyle (2001)). In both cases the model is applied for each hillslope. Finally, the discharge generated at each hillslope is routed to each associated stream link according to Mantilla and Gupta (2005) and Mandapaka et al. (2009)).

All modelling components can be calibrated using one of the calibration algorithms such as Particle Swarm Optimization algorithm (Kennedy and Eberhart (1995), Eberhart and Shi (2001)) and DREAM (Vrugt et al. (2009)). Every component can be connected, parameterized, and executed either using the OMS3 console (OMS 3.1) or the OMS3 scripting mode within the uDig Spatial Toolbox (http://code.google.com/p/jgrasstools/). Different components can be instantiated, initialized and connected in a sequence. In this way the modeler can build a custom hydrological model and solution by selecting different components to simulate the same hydrological processes. Processes will then use the OMS3 implicit parallelism to improve the computational efficiency in multicore or multiprocessor machines. The complete application of the system is presented in Formetta et al. (2011).

2. Test different modeling solutions.

As presented in Formetta et al. (2011), the Hymod component (Moore (1985) and Boyle (2001))) is applied for each HRU into which the basin is split. The rationale of using several Hymods, one for each hillslope, instead of a single one for the whole catchment as is usual in literature, was twofold: firstly, to preserve the geometrical and topological structure of the river network, which provide to embed significant information about the shape of discharge hydrograph, (D'Odorico and Rigon (2003)); and secondly, to allow the use, as input, of spatially varying rainfall and evapotranspiration fields.

Finally, the runoff production is then propagated in the channel network. In this paper, a new runoff propagation component presented. To investigate the role and possibly the importance of the channel routing component a testing is performed. Two river basins are used for test and modeled in a three different delineations by using one (DL1), three (DL3) and twenty (DL20) HRU's. Two modeling solutions are setup: Hymod and RHymod Illustrated in fig. (1).

The modeling solution RHymod includes: Pristley-Taylor component for the evapotranspiration estimate, ordinary kriging algorithm for the rainfall spatialization, hymod model for the runoff production of the hillslope and finally the new channel routing component presented in the next section. The modeling solution Hymod differs from the model solution RHymod just because the channel routing component is turned off and the discharge for each HRU is simply summed going downstream. LUCA (Hay et al. (2006)) algorithm was selected for calibrating component for both the modeling solutions. The objective function is the Kling-Gupta efficiency (KGE) function presented in Gupta et al., (2009).

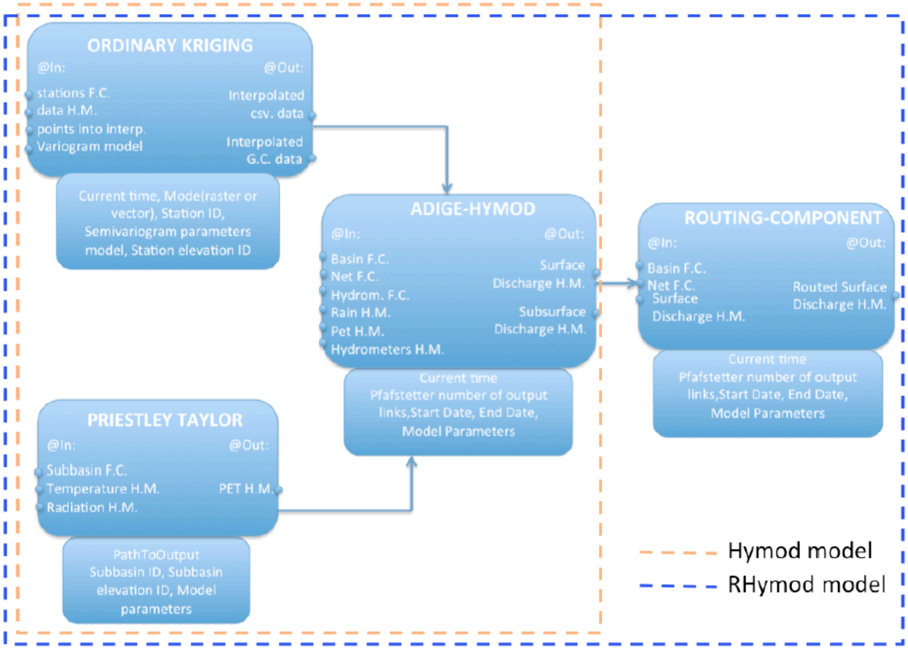

Figure 1. Modelling solutions: Hymod (in red dashed line) and RHymod (in blue dashed line).

3.1. The flow routing component.

As presented in Formetta et al. (2011) the flow generated for each hillslope is kinematically propagated downstream in the channel network by integrating, in each channel link, a non-linear variant of the Saint Venant equation (e.g. Bras and Rodriguez-Iturbe (1994)).

For each link, the continuity equation is in fact:

$$\frac{dS_i(t)}{dt} = \left[Q_{gen}(t) + \sum_{trib} Q_{trib}(t) - Q_i(t) \right] \qquad i = 1, 2, \ldots, H \tag{1}$$

where $S_i(t)$ is storage in the i-th link at time t, H is the total number of network links, $Q_i(t)$ $[L^3T^{-1}]$ is the output discharge from i-th link, $Q_{trib}(t)$ $[L^3T^{-1}]$ is the flow of upstream links, and $Q_{gen}(t)$ $[L^3T^{-1}]$ is the discharge generated at the hillslope of the link in question.

Differently from Formetta et al. (2011) the routing component is modified taking into account the novel approach proposed in Mandapaka et al. (2009). Considering a generic cross section, the relation between the storage and the output discharge from a generic i-th link is:

$$S_i(t) = \frac{Q_i(t) \cdot l_i}{v_i(t)} \tag{2}$$

in which l_i [L] and v_i [LT^{-1}] indicate, respectively, the length and the velocity in the channel i-th. The velocity is estimated as presented in Mantilla (2001):

$$v_i(t) = v_r \cdot \left(\frac{Q_i(t)}{Q_R}\right)^{\lambda_1} \cdot \left(\frac{A_i}{A_R}\right)^{\lambda_2} \qquad (3)$$

where Ai [L^2] is the upstream area of the link, v_r [LT^{-1}], Q_r [L^3T^{-1}] and A_r [L^2], are reference velocity, discharge and area, λ_1 and λ_2 are the scaling exponents of velocity for discharge and upstream area, respectively.

Replacing the velocity in eq. 2 as proposed in eq. 3 gives:

$$S_i(t) = \frac{Q_i(t) \cdot l_i}{v_r \cdot Q_i(t)^{\lambda_1} \cdot A_i^{\lambda_2}} \qquad (4)$$

where Q_r and A_r are taken to be 1 [L^3 T^{-1}] and 1 [L^2] respectively.

Deriving in time eq. 4, the left hand side of eq. 1 becomes:

$$\frac{dS_i(t)}{dt} = \frac{l_i \cdot (1-\lambda_1)}{v_r \cdot Q_i(t)^{\lambda_1} \cdot A_i^{\lambda_2}} \cdot \frac{dQ_i(t)}{dt} \qquad (5)$$

Finally, replacing eq. 5 in eq. 1, the continuity equation for the i-th link the ordinary becomes a non linear ordinary differential equation:

$$\frac{dQ_i(t)}{dt} = K\left(Q_i(t)\right) \cdot \left[Q_{gen}(t) + \sum_{trib} Q_{trib}(t) - Q_i(t)\right] \qquad (6)$$

where:

$$K\left(Q_i(t)\right) = \frac{v_r \cdot Q_i(t)^{\lambda_1} \cdot A_i^{\lambda_2}}{l_i \cdot (1-\lambda_1)} \qquad (7)$$

Eq. 6 has to be solved for each link i, i=1,2,..., H of the channel network. Using the Pfafstetter scheme as described Formetta et al. (2011) the network from upstream to downstream. Because of this reason the resolution of the set of routing equations starts from the upstream hillslopes (where the term $\sum_{trib} Q_{trib}(t)$ is null) and goes downstream (where the $\sum_{trib} Q_{trib}(t)$ becomes a known term) according to the numbering rules.

The procedure provides both the outgoing discharge and the mean velocity for each link i.

4. Application

Different components of the framework JGrass-NewAge are applied in a cascading manner according to the methodology presented in Formetta et al. (2011). In sequence they are: the geomorphological analysis tools to extract the HRU, the river network and the geomorphological features used in the other components; the meteorological interpolator components for the spatialization of the meteorological variables (air temperature and rainfall); potential evapotranspiration component; the runoff production and eventually the routing component to compute discharge; the automatic calibration component to estimate the best set of model parameters; validation package component to compute some goodness of fit indexes and to measure quantitatively the performance of the model.

For each delineation (DL1, DL3 and DL20) Hymod and RHymod modeling solutions were applied. One year calibration is performed by using the LUCA algorithm by optimizing the KGE Gupta et al. (2009) objective function. Finally the simulation results are presented both in a qualitative point of view by comparing measured and simulated hydrograph and by a quantitative point of view, by computing two indices of goodness of fit: the index of agreement, IOA, Willmott et al. (1985) and the percentage model bias (PBIAS).

The test is performed on two different river basin: Fort Cobb and Little Washita. The Little Washita river basin (611 Km**2**), (Fig.2) is located in southwestern Oklahoma, between Chickasha and Lawton.

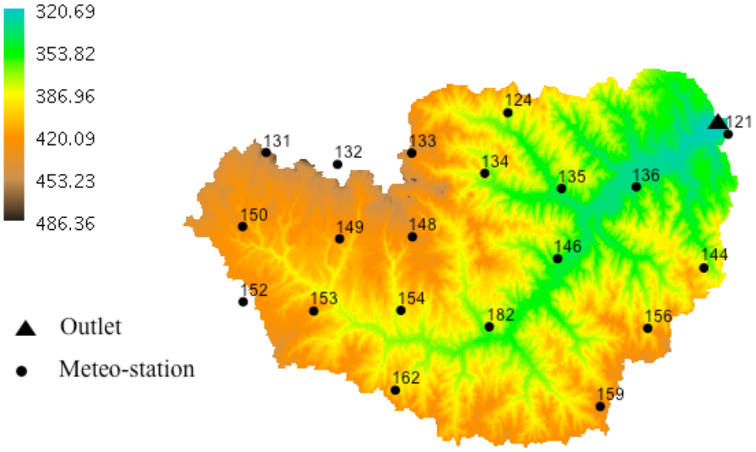

Figure 2. The Little Washita river basin, Oklahoma (U.S.A.).

The climate of the basin can be characterized as sub-humid with a long-term, spatial average, annual precipitation of 760 millimeters and a temperature of 16 degrees Celsius. Winters are typically short and dry but are usually very cold for a few weeks. Summers are typically long, hot, and relatively dry.

The elevation of the basin ranges between about 300 meters and about 500 meters a.s.l. The bedrock exposed in the watershed consists of Permian age sedimentary rocks and soil textures range from fine sand to silty loam.

The meteorological stations used in this study are plotted in black dots in fig. (2) and the hydrometer where the calibration is performed is depicted with a black triangle.

Table 1 reports the main information (coordinates and elevations) of the twenty meteorological stations (whose data are available at http://ars.mesonet.org/). Five-minute measurements of rainfall (P), air temperature (T), and incoming solar radiation (R) were aggregated to hourly time steps and used as input of the modeling system. The stream gauge measures discharge at 15-minute resolution. The values were aggregated to hourly time step and used in the automatic calibration procedure.

Table 1. List of the meteorological stations used in the simulations performed on Little Washita river basin.

ID	City	Lat	Long	Elevation	Aspect
124	Norge	34.9728	-98.0581	387	138
131	Cyril	34.9503	-98.2336	458	245
133	Cement	34.9492	-98.1281	430	116
134	Cement	34.9367	-98.0753	384	65
135	Cement	34.9272	-98.0197	366	182
136	Ninnekah	34.9278	-97.9656	343	270
144	Agawam	34.8789	-97.9172	388	50
146	Agawam	34.8853	-98.0231	358	212
148	Cement	34.8992	-98.1281	431	160
149	Cyril	34.8983	-98.1808	420	205
150	Cyril	34.9061	-98.2511	431	195
153	Cyril	34.8553	-98.2121	414	165
154	Cyril	34.8553	-98.1369	393	175
156	Agawam	34.8431	-97.9583	397	290
159	Rush	34.7967	-97.9933	439	235
162	Sterling	34.8075	-98.1414	405	15
182	Cement	34.845	-98.0731	370	245

The Fort Cobb Watershed, fig.(3), is located in the Central Great Plains Ecoregion in south-western Oklahoma in Caddo. It is 813 square kilometres in size. Its elevation ranges between 383 meters and 565 meters a.s.l. Land use in the watershed includes agricultural fields, cattle operations, rural communities, and one hog feeding operation. Most soils in the watershed are highly erodible, sandy clays and loams underlain primarily by Permian sandstone, siltstone, and claystone.

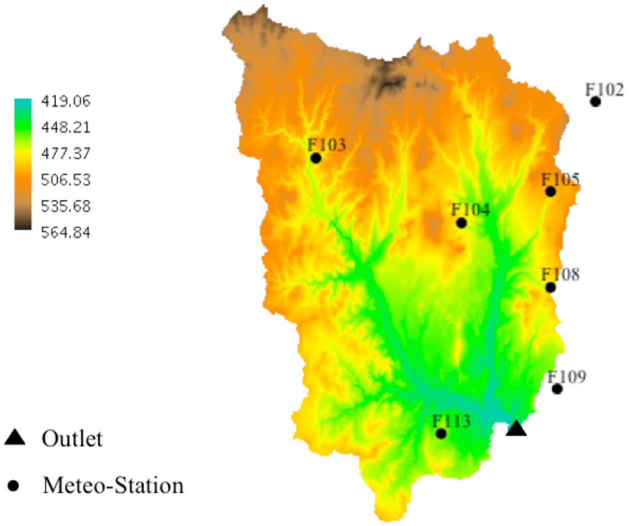

Figure 3. The Fort Cobb river basin, Oklahoma (U.S.A.).

The climate of the basin can be characterized as moist with a spatially average, annual precipitation of 816 millimeters and a temperature of 16 degrees Celsius. The JGrass-NewAGE modelling solution is applied for the Fort Cobb river basin at the Eakly outlet, before the river enters the reservoir.

Five minutes meteorological measurements of rainfall, air temperature and incoming solar radiation are available at http://ars.mesonet.org/ for the watershed. The data was aggregated to hourly time steps and used as input of the modelling system. Seven meteorological stations were used in this study. Table 2 contains their main features.

Table 2. List of the meteorological stations used in the simulations performed on Fort Cobb river basin.

ID	City	Lat	Long	Elevation	Aspect
101	Hydro	35.4551	-98.6064	504	120
104	Colony	35.3923	-98.6233	484	35
105	Colony	35.4072	-98.571	493	300
106	Eakly	35.3915	-98.5138	472	295
108	Eakly	35.3611	-98.5712	492	40
109	Eakly	35.3123	-98.5675	466	90
110	Eakly	35.3303	-98.5202	430	115
113	Colony	35.291	-98.6357	465	155
182	Cement	34.845	-98.0731	370	245

The simulation period covered the two years two years: 2006-2007 in the case Fort Cobb and 2002-2003 in the case of Little Washita river basin; one year was used for calibration and one year for verification. The simulations time step was hourly.

5. Results

The Fort Cobb and the Little Washita river basin results are presented in table 3 and 4 respectively. Each row contains: i) the delineation type (DL1, DL3 and DL20); ii) the model solution (Hymod and RHymod); iii) the optimized objective function (KGE) value and the goodness of fit indices (IOA and PBIAS) for all the simulation period.

Table 3. Fort Cobb simulation results for different delineations and for different model configurations

Delineation	Modelling solution	KGE	IOA	PBIAS
DL1	Hymod	0.53	0.79	24.4
DL1	RHymod	0.7	0.83	9.20
DL3	Hymod	0.65	0.81	13.01
DL3	RHymod	0.81	0.89	3.90
DL20	Hymod	0.63	0.8	18.4
DL20	RHymod	0.65	0.83	17.20

Table 4. Little Washita simulation results for different delineations and for different model configurations

Delineation	Modelling solution	KGE	IOA	PBIAS
DL1	Hymod	0.69	0.81	16.50
DL1	RHymod	0.74	0.85	7.30
DL3	Hymod	0.76	0.84	9.00
DL3	RHymod	0.82	0.89	3.02
DL20	Hymod	0.76	0.85	8.40
DL20	RHymod	0.77	0.84	7.60

Tables 5 and 6 present the optimum values of the model parameters for both the model configurations (Hymod and RHymod) and for all the delineations (DL1, DL3 and DL20), respectively for Fort Cobb and Little Washita river basin.

From the quantitive analysis of the results it can be concluded that both modeling solutions, Hymod and RHymod, are able to simulate in a reliable way the discharge. Based on the goodness of fit indices, the total volume is actually better simulated using RHymod than Hymod model. In fact in the RHymod case the PBIAS shows lower values both for the Fort Cobb and for the Little Washita river basin. Moreover, the RHymod model is able to simulate both the peak values and the peak time, as is confirmed by better KGE and IOA values than Hymod in both the study cases.

Table 5. Fort Cobb river basin: parameter sets used in the simulations for RHymod (RH) and Hymod (H) model for different delineations (DL1, DL3 and DL3

Symbol	DL1-H	DL1-RH	DL3-RH	DL3-RH	DL20-H	DL20-RH
C_{max}	906.05	403.80	141.3387	813.29	696.25	595.02
B_{exp}	1.7392	0.7204	2.1321	1.2697	1.1917	2.207
Alpha	0.2193	0.2487	0.1294	0.23	0.3616	0.3619
R_q	0.2261	0.3587	0.2088	0.2099	0.2288	0.2207
R_s	0.0008	0.0007	0.0001	0.0009	0.0012	0.0011
v_r	-	0.3132	-	0.6594	-	0.5806
λ_1	-	0.7978	-	-0.3915	-	-0.5298
λ_2	-	0.0750	-	0.842	-	0.3420

Table 6. Little Washita river basin: parameter sets used in the simulations for RHymod (RH) and Hymod (H) model for different delineations (DL1, DL3 and DL3

Symbol	DL1-H	DL1-RH	DL3-RH	DL3-RH	DL20-H	DL20-RH
C_{max}	841.83	520.70	155.83	635.16	998.93	743.31
B_{exp}	1.2597	1.2449	1.9143	5.6479	3.637	2.5734
Alpha	0.2675	0.4501	0.2122	0.2526	0.2669	0.254
R_q	0.1259	0.4357	0.1202	0.4882	0.1338	0.136
R_s	0.0039	0.0006	0.0003	0.0002	0.0048	0.0048
v_r	-	1.187	-	0.5449	-	0.5964
λ_1	-	0.09	-	-0.0323	-	0.2262
λ_2	-	-0.0703	-	-0.0215	-	0.115

On the other hand, the RHymod model has three more parameters than Hymod. It brings to increase the calibration convergence time and the optimal parameter spotting with respect to Hymod model that also provided acceptable results.

For both the river basins, the RHymod model, where the channel routing is explicit, provides better performances in the delineation DL3. The models' performances decrease in the case of delineation DL1. Even if RHymod outperformed Hymod model, this could be due to neglecting the rainfall spatial variability: a spatially uniform rainfall is applied in this case. In the case of the DL20 delineation, the use of RHymod and the explicit routing model did not provide any model performance improvement. This happened in both the river basins. This result confirms the findings of in D'Odorico and Rigon (2003) and Botter and Rinaldo (2003) where it is evidently shown that the hillslope (and not the channel) contribute with the largest part of the residence time. In the DL20 delineation HRU's size is the smallest. Moreover, at this scale, for both the basins up to 15-25 km^2 , non linearity in the process of runoff production could not be simulated well by a model based on linear reservoir (such as Boyle (2001))

Both models, slightly underestimated the highest peak flood values. This could be due to the fact that non-specific calibrations were performed for these events and to the implicit assumptions made in the classical formulation of Hymod Moore (1985) where residence time in the hillslopes does not depend on the soil moisture conditions. This is not in total agreement with what it is known of the hydrological problem and a possible solution could be the use of non-linear runoff generation models instead the linear model presented in this study.

6. Conclusions

The JGrass-NewAge system provides not only a new hydrological tool but a system in which any model can be built in components that can be independently modified or changed. In this paper a verification of single parts of a modeling chain, keeping the others fixed, is performed. A new channel routing component is presented. Hymod and RHymod hydrological models were set up: in Hymod, no routing component is used, and in RHymod, the new routing component is used. The two different modeling solutions are tested on Little Washita and Fort Cobb river basins and discharge simulations are performed. The basin delineation is also varied in order to understand the effect of the HRUs size.

Results show that the RHymod improved, even though not dramatically, the model results in terms of discharge simulation. The model with the routing component performed best in the case of middle size HRUs (DL3). In the case of small size HRUs (DL20) there are no significant differences between the two modeling solutions.

The paper finally shows the possibility of a component by component and interoperability comparison on the same framework. For example the JGrass- NewAge system could be compared with others models, such as PRSM (Leavesley et al. (1983)) or J2000 (Krause (2001)) that embraced the OMS3 framework.

References

Antevs, E., 1954: Climate of New Mexico during the last glacio-pluvial. *J. Geology*, **62**, 182-191.

Bailey, R. W., 1935: Epicycles of erosion in the valleys of the Colorado Plateau province. *J. Geology*, **43**, 337-355.

Balling, R. C., and S. G. Wells, 1990: Historical rainfall patterns and arroyo activity within the Zuni River drainage basin, New Mexico. *Ann. Assoc. Amer. Geog.*, **80**(4), 603-617.

Allen, R., Pereira, L., Raes, D., Smith, M., et al.: Crop evapotranspiration-Guidelines for computing crop water requirements-FAO Irrigation and drainage paper 56, FAO, Rome, 300, 6541, 1998.

Bird, R. and Hulstrom, R.: Simplified clear sky model for direct and diffuse insolation on horizontal surfaces, Tech. rep., Solar Energy Research Inst., Golden, CO (USA), 1981.

Botter, G. and Rinaldo, A.: Scale effect on geomorphologic and kinematic dispersion, Water resources research, 39, 1286, 2003.

Boyle, D. P.: Multicriteria calibration of hydrological model, Ph.D. dissertation, Dep. of Hydrol. and Water Resour., Univ. of Ariz., Tucson, 2001.

Bras, R. and Rodriguez-Iturbe, I.: Random functions and hydrology, Dover Pubns, 1994.

Brutsaert, W.: Evaporation into the atmosphere: Theory, history, and applications, vol. 1, Springer, 1982.

Brutsaert, W.: Hydrology: an introduction, Cambridge Univ Pr, 2005.

Corripio, J.: Modelling the energy balance of high altitude glacierised basins in the Central Andes., PhD dissertation, University of Edinburgh; 2002, 2002.

Cressie, N.: Statistics for spatial data, Terra Nova, 4, 613{617, 1992.

David, O., Ascough, J., Leavesley, G., and Ahuja, L.: Rethinking modeling framework design: object modeling system 3.0, in: Environmental Modelling International Conference Proceedings, pp. 5-8, 2010.

D'Odorico, P. and Rigon, R.: Hillslope and channel contributions to the hydrologic response, Water resources research, 39, 1113, 2003.

Duffy, C. J.: A Two-State Integral-Balance Model for Soil Moisture and Groundwater Dynamics in Complex Terrain, Water Resour. Res., 32, 2421{2434, URL http://dx.doi.org/10.1029/96WR01049 , 1996.

Eberhart, R. and Shi, Y.: Particle swarm optimization: developments, applications and resources, in: Proceedings of the 2001 congress on evolutionary computation, vol. 1, pp. 81-86, Piscataway, NJ, USA: IEEE, 2001.

Erbs, D., Klein, S., and Due, J.: Estimation of the diffuse radiation fraction for hourly, daily and monthly-average global radiation, Solar Energy, 28, 293-302, 1982.

Formetta, G., Mantilla, R., Franceschi, S., Antonello, A., and Rigon, R.: The JGrass-NewAge system for forecasting and managing the hydrological budgets at the basin scale: models of flow generation and propagation/routing, Geoscientific Model Development, 4, 943-955, doi:10.5194/gmd-4-943-2011, URL http://www.geosci-model-dev.net/4/943/2011/ , 2011.11

Garen, D. and Marks, D.: Spatially distributed energy balance snowmelt modelling in a mountainous river basin: estimation of meteorological inputs and verification of model results, Journal of Hydrology, 315, 126-153, 2005.

Garen, D., Johnson, G., and Hanson, C.: Mean areal precipitation for daily hydrologic modeling in mountainous regions1, JAWRA Journal of the American Water Resources Association, 30, 481-491, 1994.

Goovaerts, P.: Geostatistics for natural resources evaluation, Oxford University Press, USA, 1997.

Gupta, H., Kling, H., Yilmaz, K., and Martinez, G.: Decomposition of the mean squared error and NSE performance criteria: Implications for improving hydrological modelling, Journal of Hydrology, 377, 80-91, 2009.

Hay, L., Leavesley, G., Clark, M., Markstrom, S., Viger, R., and Umemoto, M.: Step wise, multiple objective calibration of a hydrologic model for a snowmelt dominated basin1, JAWRA Journal of the American Water Resources Association, 42, 877-890, 2006.

Helbig, N., Lowe, H., Mayer, B., and Lehning, M.: Explicit validation of a surface shortwave radiation balance model over snow-covered complex terrain, Journal of Geophysical Research Atmospheres, 115, D18 113, 2010.

Iqbal, M.: An introduction to solar radiation, 1983.

Kennedy, J. and Eberhart, R.: Particle swarm optimization, in: Neural Networks, 1995. Proceedings., IEEE International Conference on, vol. 4, pp. 1942-1948, IEEE, 1995.

Krause, P.: Das hydrologische Modellsystem J2000: Beschreibung und Anwendung in grofen Flufegebieten, Forschungszentrum, Zentralbibliothek, 2001.

Leavesley, G., Lichty, R., Troutman, B., and Saindon, L.: Precipitation-runoff modeling system: User's manual, Available from Books and Open File Report Section, USGS Box 25425, Denver, Co 80225. USGS Water Resources Investigations Report 83-4238, 1983. 207 p, 54 _g, 15 tab, 51 ref, 8 attach., 1983.

Lloyd, C.: Assessing the effect of integrating elevation data into the estimation of monthly precipitation in Great Britain, Journal of Hydrology, 308, 128-150, 2005.

Mandapaka, P., Krajewski, W., Mantilla, R., and Gupta, V.: Dissecting the effect of rainfall variability on the statistical structure of peak flows, Advances in Water Resources, 32, 1508-1525, 2009.

Mantilla, R.: Physical basis of statistical self-similarity in peak flows on random self-similar networks, PhD dissertation, University of Colorado, Boulder; 2007, 2001.

Mantilla, R. and Gupta, V.: A GIS numerical framework to study the process basis of scaling statistics in river networks, IEEE Geoscience and Remote Sensing Letters, 2, 404{408, 2005.12

Monteith, J. et al.: Evaporation and environment, in: Symp. Soc. Exp. Biol, vol. 19, pp. 205{234, 1965.

Moore, R.: The probability-distributed principle and runoff production at point and basin scales, Hydrol. Sci. J., 30, 165, 1985.

Orgill, J. and Hollands, K.: Correlation equation for hourly diffuse radiation on a horizontal surface, Solar energy, 19, 357{359, 1977.

Penman, H.: Natural evaporation from open water, bare soil and grass, Proceedings of the Royal Society of London. Series A. Mathematical and Physical Sciences, 193, 120{145, 1948.

Priestley, C.: Turbulent transfer in the lower atmosphere, University of Chicago Press Chicago, Ill., 1959.

Priestley, C. and Taylor, R.: On the assessment of surface heat flux and evaporation using large-scale parameters, Monthly weather review, 100, 81-92,1972.

Reindl, D., Beckman, W., and Du_e, J.: Di_use fraction correlations, Solar Energy, 45, 1-7, 1990.

Slatyer, R. and McIlroy, I.: Practical Microclimatology., Practical Microclimatology., 1961.

Vrugt, J., Ter Braak, C., Diks, C., Higdon, D., Robinson, B., and Hyman, J.:
Accelerating Markov chain Monte Carlo simulation by di_erential evolution with self-adaptive randomized subspace sampling, International Journal of Nonlinear Sciences and Numerical Simulation, 10, 273-290, 2009.

Willmott, C., Ackleson, S., Davis, R., Feddema, J., Klink, K., Legates, D., ODonnell, J., and Rowe, C.: Statistics for the evaluation and comparison of models, Journal of Geophysical Research, 90, 8995{9005, 1985.13